

An Orbital House of Cards: Frequent Megaconstellation Close Conjunctions

Sarah Thiele^{1*}, Skye R. Heiland², Aaron C. Boley², Samantha M. Lawler³

¹Department of Astrophysical Sciences, Princeton University.

²Department of Physics and Astronomy, University of British Columbia.

³Campion College and the Department of Physics, University of Regina.

*Corresponding author(s). E-mail(s): sarah.thiele@princeton.edu;

Abstract

The number of objects in orbit is rapidly increasing, primarily driven by the launch of megaconstellations, an approach to satellite constellation design that involves large numbers of satellites paired with their rapid launch and disposal. While satellites provide many benefits to society, their use comes with challenges, including the growth of space debris, collisions, ground casualty risks, optical and radio-spectrum pollution, and the alteration of Earth’s upper atmosphere through rocket emissions and reentry ablation. There is potential for current or planned actions in orbit to cause serious degradation of the orbital environment or lead to catastrophic outcomes, highlighting the urgent need to find better ways to quantify stress on the orbital environment. Here we propose a new metric, the CRASH Clock, that measures such stress in terms of the timescale for a possible catastrophic collision to occur if there are no satellite manoeuvres or there is a severe loss in situational awareness. Our calculations show the CRASH Clock is currently 5.5 days, which suggests there is limited time to recover from a wide-spread disruptive event, such as a solar storm. This is in stark contrast to the pre-megaconstellation era: in 2018, the CRASH Clock was 164 days.

1 Introduction

The long-term sustainable use of satellites in Earth orbit requires an ongoing effort by all operators to limit the negative impacts of their actions. With this, there has long been a recognized need for identifying environmental targets and metrics. One example is the so-called 25-year rule (now being reduced to five years by some regulators), which sets an upper limit to the desired post-mission orbital lifetime of low Earth orbit (LEO) satellites in an effort to avoid producing debris from collisions [1, 2]. A related example is the post-mission disposal (PMD) success rate, a measure of removing objects from

orbit after their mission ends (see discussions regarding target PMD success rates in e.g. [3]¹). This metric is often used to help parametrize long-term evolution models of Earth’s satellite environment. The level of adherence by operators to PMD targets can strongly influence orbital debris evolution [4, 5].

A more wide-reaching way to measure environmental stress on orbit is to identify an orbital carrying capacity, which broadly seeks to answer the question of how many things can be safely placed in orbit. The problem is that carrying capacity is not an inherently well-defined metric because it may depend on tolerances for damage, how the satellites are maintained, and the types of objects in orbit. An example of a proposed measure for carrying capacity is the χ metric (or “ χ -capacity”) [6], which is a ratio of the number of satellites in orbit at equilibrium (accounting for collisions) to the ideal (non-collisional) number. Another that calculates the maximal satellite population associated with a stable equilibrium debris population is the instantaneous Kessler capacity (IKC) [7]. Others have been proposed, and we do not attempt to summarize them all.

Key environmental indicators (KEIs) offer a complementary approach by using metrics that are clearly defined and do not depend on specific use cases. Instead, they indicate the current orbital conditions and characterize stress (e.g., levels of orbital degradation and fragility) rather than capacity. Moreover, KEIs offer valuable tools for creating effective policies to address complex issues, such as the Sustainable Development Goal indicators [8]. The measured PMD rate is an example of a KEI. Tracking how many satellites are visible above the horizon, averaged across the Earth as proposed by [9] is a metric that might be interpreted as a KEI using our language. A symbiotic approach to this KEI framework is the concept of orbital “health” indicators, proposed in [10], which also includes the raw counts of artificial objects in space as a proposed indicator.

In some cases there is little distinction between the way carrying capacity is defined and how we use KEIs, such as when carrying capacity is used as a reference point to define consumption levels, creating a measurable proxy for orbital degradation. For example, [5] uses a globally integrated debris index as a measure of environmental capacity and its consumption, and propose using a maximum increase in this cumulative index compared to some reference epoch as a recommended ceiling.

The use of KEIs can further help to provide a suite of metrics for exploring when nonlinearities could occur or where there could be system-wide effects (such as across LEO). As an example, the concept of Kessler-Cour-Pallais Syndrome (KCPS) [11] is made evident by KEIs (e.g., critical densities or collision area). KCPS is a condition in which the growth of collisional debris (and surface area) on orbit outpaces debris removal through atmospheric drag, causing a collisional runaway. However, despite the use of the term “runaway”, the initial phase of KCPS (which some argue we have already entered, see e.g. [12]) is characterized by slow growth of debris, taking decades to centuries to develop. Such long timescales create a challenge for using the idea of KCPS alone as a policy tool.

While a KEI framework does not require the identification of a maximum stress, it does help to conceptualize a stress spectrum – where there is an acceptable range, an unknown range, and a clearly unacceptable range. This is helpful, as determining hard

¹Note that there are several definitions of PMD rates, applied in difference contexts.

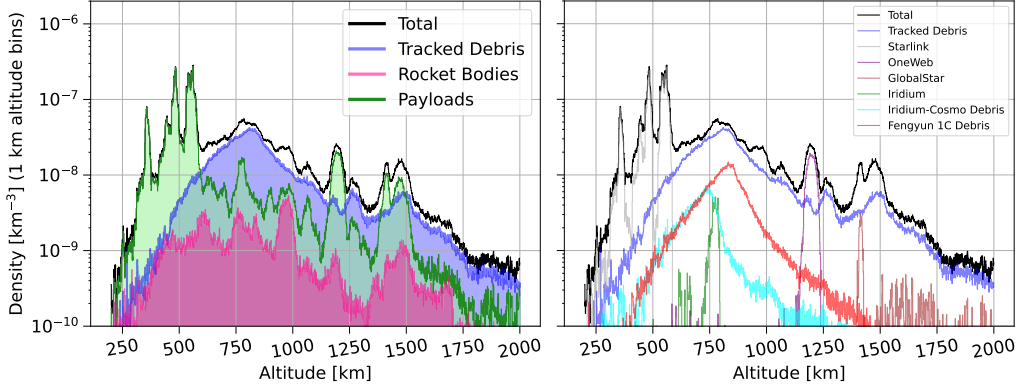


Fig. 1 Orbit-averaged volume density distribution of RSOs by classification (left) and origin (right) as of 25 June 2025. Left: ‘Payload’ refers to active and defunct satellites, ‘Tracked Debris’ only those debris pieces that are reliably tracked in the debris catalogue, excluding abandoned rocket bodies and defunct satellites. Right: Densities of active constellations and megaconstellations, as well as tracked debris, debris from the 2009 Iridium-Cosmos collision, and debris from the 2007 Fengyun 1C ASAT test.

limits within a KEI framework is not a well-defined task, as discussed above. Indeed, for some KEIs, a clear threshold may not exist.

A KEI framework further provides a way to avoid shifting baseline syndrome (SBS) [13]. SBS describes the sociological and psychological phenomenon in which the acceptable baseline for environmental conditions degrades over time. It is therefore important to compare the current state of LEO not just to that of the era before megaconstellations, but to the pristine orbital environment that existed decades ago². Our tolerance for on-orbit risks should be calibrated with the very beginning of space exploration as its zero-point. Attempts should be made to counteract the bias of growing up with an already-littered orbit when setting space sustainability metric targets.

With this in mind, we introduce the Collision Realization And Significant Harm (CRASH) Clock, a KEI that evaluates the stress on the orbital environment. Many simulations predicting collision rates on orbit assume perfect collision avoidance for all manoeuvrable payloads during their operational lifetimes (e.g. Section 7.2 of [15], [16]). In contrast, the CRASH Clock uses the known distribution of resident space objects (RSOs: active and derelict satellites, debris, and rocket bodies) to determine how quickly we could expect a collision if all manoeuvres were to suddenly stop or if there was a severe loss in situational awareness (such as due to a major solar storm or catastrophic software issue). It is a measure, in part, of the degree to which the orbital environment is a house of cards.

2 Results

We start by exploring the current number density distribution for different types of RSOs (shown in Fig. 1), based on the two-line elements (TLEs) for 25 June 2025, averaged over spherical shells (see Methods). Because objects are not randomly distributed in their orbital inclination, the resulting densities should be interpreted as averages, with the understanding that there can be substantial variation in local densities.

²Though outside the scope of this work, we note that this concept applies even more so to orbital light pollution and Dark and Quiet Sky protection [14].

Starlink satellite shells exhibit the highest densities on orbit, reaching over an order of magnitude higher than the tracked space debris peak at approximately 800 km altitude, which has large contributions from the 2007 Chinese anti-satellite weapon test (Fengyun 1C) and the 2009 Iridium 33-Kosmos 2251 collision.

Using this density distribution, we can calculate expectations for close encounter rates among RSOs, as well as collisions under the assumption of no manoeuvres. The satellite-satellite encounter/collision rate is approximated by

$$\Gamma_{\text{sat}} = \frac{1}{2} \int_V n_{\text{sat}}^2 A_{\text{col}} \bar{v}_r dV, \quad (1)$$

where n_{sat} is the number density of satellites at some altitude, A_{col} is the encounter-/collision cross-section of the satellites, \bar{v}_r is the typical relative collision speed, and dV is the spherical volume element. The factor of 1/2 is to ensure an encounter between two objects of the same population is not counted twice. This encounter/collision rate can naturally be extended to include combinations of various RSOs (e.g., debris-satellite, debris-debris), as well as non-trivial distributions of collisional area. We also assume that the satellites are randomly distributed within a shell.

To demonstrate the consequences of Figure 1, we can integrate Equation 1 over a limited volume. As an illustrative example, let us integrate over the peak in the density distribution centred on 550 km altitude, assuming a uniform spherical shell. We approximate the shell as being 30 km thick from the peak's width, and assume a possible collision cross section of $A_{\text{col}} \approx 300 \text{ m}^2$, corresponding to a close approach of 10 metres. While such a close approach does not guarantee a collision, depending on the orientation of the satellites involved, it could lead to one, and we use the term “collision” moving forward. Indeed, the average collision distance for randomly oriented thin rods of full length L is approximately $0.3L$. As such, thin satellites but with 30 m solar panel spans can have very large effective cross sections, should there be a loss of control of their orientations. From a safety point of view, using an average physical area for the satellite would underestimate the collision cross section, possibly severely. We discuss this further in Methods.

As also discussed in Methods, we use $\bar{v}_r \approx 10 \text{ km s}^{-1}$. The density appears to peak at $n_{\text{sat}} \approx 3 \times 10^{-7} \text{ km}^{-3}$, but upon closer inspection we find that the density finely oscillates around $n_{\text{sat}} \approx 2 \times 10^{-7} \text{ km}^{-3}$, so we use this latter value as the average density in the shell.

For the given altitude, the single shell collision rate is thus $\Gamma_{\text{ss}} \approx 2.2 \times 10^{-6} \text{ s}^{-1}$ or about 0.09 d^{-1} . Defining the single shell expectation time between collisions to be $\tau_{\text{ss}} = 1/\Gamma_{\text{ss}}$, we find $\tau_{\text{ss}} \approx 11 \text{ d}$. This means that the timescale for a 50% chance of one or more potential collisions is about $t \approx 7.6 \text{ d}$ in that shell alone, assuming a Poisson process, i.e. probability $P = 1 - \exp(-t/\tau_{\text{ss}})$. This result, while approximate, emphasizes that the collision probability for satellites on orbit is substantial without active management.

Although spherical shells around Earth represent extremely large volumes and the instantaneous volume occupied by satellites is small, LEO satellites orbit the Earth in approximately 90 minutes depending on the altitude. As a result, these satellites quickly

explore their mutual interaction possibilities. Collision avoidance manoeuvres and station-keeping (i.e. manoeuvres to maintain desired altitudes, separations and orbital phasing), are essential in dense satellite shells and successful active management of constellations seems to be the only reason why there has not been a recent major satellite-satellite collision as orbital densities continue to increase. We will revisit the importance of station-keeping further below.

Now we extend our calculation to include all RSO interactions, throughout all of LEO. Let the expected rate of close encounters less than 1 km in distance (i.e. $A = \pi \text{ km}^2$) within spherical shells of altitude h be given by $\Gamma_{1,h}$. We choose a conjunction distance of 1 km because it roughly corresponds to the distance at which a collision avoidance manoeuvre is executed. In practice, such manoeuvres do not depend on a fixed distance; rather, they occur when the probability of a collision exceeds a risk tolerance threshold (e.g. [17]), which varies between operators. That probability is further dependent on the uncertainties of the orbits in question. We avoid these complexities by using the 1 km approach distance as an imperfect proxy.

With this in mind, the corresponding encounter time within each spherical shell is $\tau_{1,h} = 1/\Gamma_{1,h}$. The blue curve shows this result in Figure 2, using the density distribution from Figure 1. In the densest part of Starlink's 550 km orbital shell, we expect close approaches (< 1 km) every 22 minutes in that shell alone.

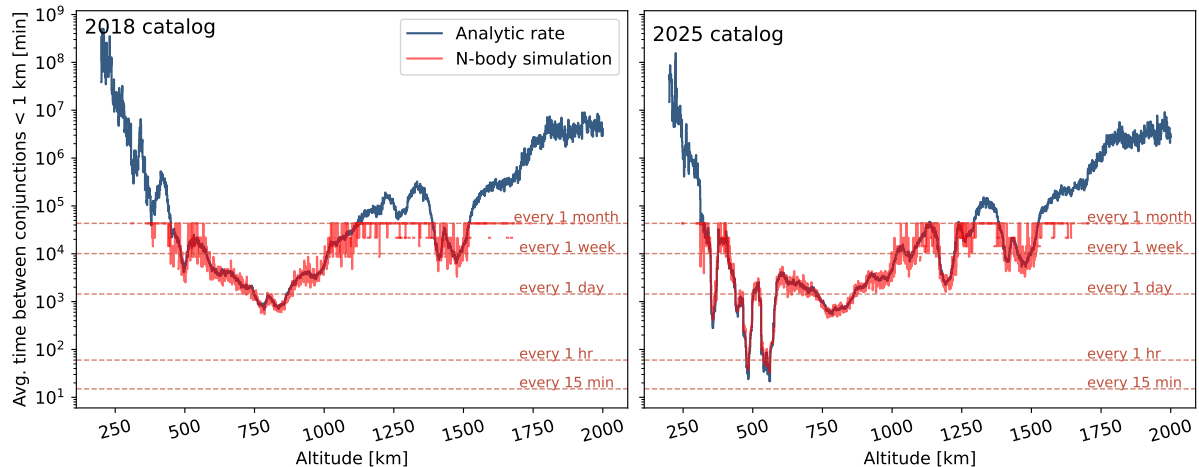


Fig. 2 Average time between conjunctions < 1 km as a function of altitude for the 2018 (left) and 2025 (right) RSO populations. The dips around 500 km correspond to the peaks in RSO density at the same altitude presented in Figure 1 due to Starlink. Our analytic calculation is shown in dark blue, with the simulations overlaid in red. The simulation duration was one month.

The time between < 1 km close encounters for all of LEO is found by summing over the rates, with $\tau_1 = (\sum_h \Gamma_{1,h})^{-1}$. For all objects, Equation 1 gives $\tau_1 = 36$ seconds. This is dominated by encounters involving at least one satellite (i.e. Sat-RSO encounters), with Starlink (the primary operator in orbit) satellites making up the majority of the satellite population. For Sat-RSO encounters, $\tau_1 \approx 41$ s, while for Starlink-RSO, $\tau_1 \approx 47$ s.

According to the most recent SpaceX biannual report, Starlink satellites made 144,404 collision avoidance manoeuvres in the period between 1 Dec 2024 and 31 May 2025 [17], averaging to 41 manoeuvres per satellite per year, or one collision avoidance manoeuvre

every 1.8 minutes across the whole megaconstellation. Keeping in mind that our encounter distance does not directly translate to a collision probability threshold for manoeuvres, nor do we take into account the effects of station-keeping, we interpret the Starlink manoeuvre time to indicate that our simulation results and analytic calculations (1.1 min and 47 s, respectively, see Methods and following discussion regarding our simulations) are reasonable for a no-manoeuvre situation.

2.1 The CRASH Clock

Taking the estimates above one step further, we can approximate the time for close approaches that could give rise to collisions on orbit. We propose this approach as a measure of the stress in orbital space: the CRASH Clock. For this calculation, we must make some assumptions about collision cross sections.

We use our previously calculated RSO number density distributions as described in Methods, but keep the densities separated into categories (i.e. the number density in a given shell is the sum of n_{debris} , n_{sat} , etc.). Each interaction combination is then assigned a “collision” cross section (described in Methods). For this discussion, we take collisions to become possible whenever the centre-centre distance between two objects is 10 m (satellite-satellite; rocket body-satellite), 5 m (satellite-debris; rocket-body debris), and 10 cm (debris-debris), although different cross sections could be used.

The total collision rate for a given altitude is

$$\Gamma_h = \bar{v}_r V_h \sum_{i,j \leq i} \left(1 - \frac{1}{2} \delta_{ij}\right) n_i n_j A_{ij}^{\text{col}} \quad (2)$$

for object types i and j , shell volume V_h and average relative speed $\bar{v}_r = \bar{v}_r(h)$. Terms with $i = j$ are halved as in Equation 1. The corresponding collision time is found by summing the rates over all of LEO. For our June 2025 catalogue, this is about $\tau_{\text{col}} = 5.5$ d – the CRASH Clock value for that date. For comparison, the no-manoeuvre collision time for Starlink-RSO collisions is about 6 d. Said differently, if all types of manoeuvres were to suddenly stop, and with our assumptions for collision cross-sections, within 24 hours there is a 17% chance of a close approach that could lead to a collision between two catalogued RSOs, with a 15% that the interaction would involve a Starlink satellite, assuming a Poisson process. Such collisions would be catastrophic, causing a major debris-generating event with high likelihood of secondary and tertiary collisions due to high orbital densities and local collision areas. We repeat this calculation using the LEO TLE catalogue from 1 January 2018, providing a reference value from prior to the megaconstellation era. In stark contrast, the CRASH Clock was 164 days, corresponding to less than a 1% chance of a collision happening between two RSOs within 24 hours under no-manoeuvre conditions. Different CRASH Clock values for different cross sections are discussed further in Methods.

The fidelity of our analytic calculations is compared to direct N-body simulations (see Methods). Simulations were initialized using TLEs for two different epochs: 1 January 2018, and 25 June 2025. The red curves in Figure 2 show the average time between conjunctions less than 1 km as a function of altitude, which shows very good agreement

Table 1 Results for our analytic and simulated close encounter times. We show results for both our 2018 and 2025 epochs, for encounter distances d within 1 km and 100 m, as well as our CRASH Clock value for each epoch. Our simulations and analytic calculations agree to within a factor of two.

	2018, analytic	2018, sim	2025, analytic	2025, sim
$d < 1$ km, all LEO	3.9 min	3.5 min	36 s	44 s
$d < 1$ km, Sat–RSO	12.4 min	11.0 min	41 s	53 s
$d < 100$ m, all LEO	6.6 hr	5.2 hr	60 min	42 min
$d < 100$ m, Sat–RSO	20.7 hr	10.5 hr	69 min	56 min
CRASH Clock	164 d		5.5 d	

with the analytical estimate. Recall that the analytic simulations assume random orbital configurations within each shell, while the simulations use the actual orbits. At least for counting close conjunctions in a statistical sense, our assumption of a random distribution does not appear to be a limitation of the analytic approach. The left-hand panel of Figure 2 shows the 2018 distribution, the right-hand shows 2025. We see that the minimum time between conjunctions has decreased by about two orders of magnitude between 2018 and 2025.

Both the simulations and the analytic calculations are intended to represent encounter statistics for a snapshot in time, akin to a steady state system. That is, we make our calculations using only a chosen TLE catalogue epoch and do not incorporate evolution of the objects on orbit through launches, active debris removal, or PMD. We note that our simulations also do not incorporate atmospheric drag, which would serve to clear out debris at lower altitudes, decrease satellite altitudes, and potentially increase the rate at which satellite orbits would randomize without station-keeping efforts in place.

Additional simulation runs were carried out on these populations using a much smaller time-step (see Methods) and a conjunction distance threshold of 100 m to search for conjunction events that could give rise to a collision. For the 25 June 2025 TLEs, we see a 100 m conjunction frequency of approximately 1 encounter every 42 minutes, within a factor of two of the analytic estimate (expecting approximately 1 encounter every 60 minutes for distances less than 100 m). For this particular simulation initialization, a conjunction less than 30 metres occurs in the first 3 hours between debris and a satellite. While this is not inherently a collision, it is an extreme encounter. We note that there is some difficult-to-characterize uncertainty in these numbers because we are using only a single simulation initialization. We have summarized all of our results for both TLE catalogue epochs in Table 1.

3 Discussion

Simulations have shown that altitudes above 600–800 km altitude in LEO are already above the unstable threshold for long-term runaway debris growth, i.e., KCPS [18, 19].

Strikingly, given the density and surface area, the main Starlink shell (about 550 km altitude) is also within the runaway threshold [19], meaning a single collision could have catastrophic long-term consequences. While collisional cascades can take decades to centuries to develop, a single collision could create substantial stress on the orbital environment immediately, even if it does not lead to a runaway [20, 21].

In an effort to better characterize this stress, for both short and long-term consequences, we recommend the CRASH Clock, which is the expectation time for a collision if all satellite manoeuvres were to suddenly stop. It is a KEI calculated using the methods above, and provides an immediate assessment, as well as historical record, of the stress on the orbital environment. It further provides a measure of the typical time between system-wide loss of control in LEO and a possible catastrophic collision.

We find that our simulations and analytic calculation yield consistent results to within a factor of two. For the purpose of determining the CRASH Clock value, we recommend using the analytic method, even though it assumes randomized orbits. There are several reasons for this. First, the analytic approach is an accessible calculation that only requires a TLE catalogue. Second, it avoids differences in the results that could arise from the choice of numerical methods. Third, simulation techniques could suffer from substantial statistical variation, potentially requiring many simulation initializations. Indeed, such variation can already be seen in the simulation results presented here.

Station-keeping and constellation design deserve a special mention. Satellite constellations can be designed to minimize conflicting interactions among their satellites, with station-keeping being done to maintain optimal configurations [see e.g. 22–24]. We can thus contemplate situations in which we have ideal constellation designs. In such cases, the CRASH Clock value could in practice be modified to take into account the “phase mixing” time of the constellation in question; by phase mixing time, we mean the theoretical time it would take for the constellation’s orbits to randomize in phase. However, we emphasize again that our analytics and simulations are in reasonable agreement, the latter of which takes into account a snapshot of actual constellation configurations. For this reason, we recommend against removing constellations with idealized designs when determining the CRASH Clock value.

Currently, the 10m-5m-10cm CRASH Clock in LEO is 5.5 days. Yet, the probabilistic nature of collisions means they could happen sooner than any given CRASH Clock value (again in the absence of manoeuvres). Recall that our example numerical simulations showed a debris-satellite conjunction of less than 30 metres in the first 3 hours of simulation time.

We emphasize that the CRASH Clock does not measure the onset of KCPS, nor should it be interpreted as indicating a runaway condition. However, it does measure the degree to which we are reliant on errorless operations. In the short term, a major collision is more akin to the Exxon Valdez oil spill disaster [25] than a Hollywood-style immediate end of operations in orbit. Indeed, satellite operations could continue after a major collision, but would have different operating parameters, including a higher risk of collision damage.

A CRASH Clock value of less than a week is already a reason for concern, as major solar storms, such as the May 2024 Gannon storm, can have lingering impacts for the satellite population. For example, in the three days of this storm, nearly half of all active LEO satellites manoeuvred due to increased atmospheric drag to maintain their orbits, and the unpredictable drag in addition to bulk manoeuvring made collision assessment during and after the storm very difficult [26, 27]. Additionally, in such conditions positional uncertainties can easily become as high as several km [28], making collision avoidance manoeuvres extremely uncertain. Moreover, while the May 2024 storm was the strongest geomagnetic storm in decades, The Great Geomagnetic Storm of 1859 was at least twice as intense [29, 30]. That event was characterized by two strong storms within a few days of each other, with the latter commonly known as the Carrington Event (September 1859). The storm peaks lasted for several hours, while the storm durations were for a day and several days, respectively [31].

The number of collision avoidance manoeuvres made by Starlink has historically been doubling every six months [32], although this seems to be the result of several factors, including lowering their risk thresholds (i.e., increasing safety practices). Each manoeuvre can create uncertainty in the estimated satellite positions, with one study even finding inaccuracies immediately after the manoeuvre of up to 40 km [33]. As the number of required manoeuvres continues to increase, temporary lapses in collision avoidance capabilities, whether that be from inaccurate orbital determination or even a small miscommunication between operators in manoeuvre decision-making, will become increasingly catastrophic in their potential consequences. Indeed, in 2019 an ESA satellite was forced to manoeuvre out of the way of a Starlink satellite when a bug in SpaceX's alert system prevented them from seeing an increased collision probability [34]. Before modern space traffic management policies, insufficient manoeuvre plan information between operators was the main cause that led to the Iridium-Cosmos collision of 2009 [35].

The Guidelines for the Long-Term Sustainability of Outer Space Activities of the United Nations Committee on the Peaceful Uses of Outer Space took the important step of identifying Earth's orbit as a finite resource [36]. Placing a satellite into orbit is resource consumption; debris, abandoned rocket bodies, and derelict spacecraft all lock up resources without any benefits. However, numbers of objects alone provide insufficient information. Collisional surface area and timely updates to published orbits are also needed. The CRASH Clock is, in part, a measure of the consumption of Earth's orbital space and the degree to which operations there are being done sustainably. Increases in either orbital density or collisional cross section decreases the collision time on orbit, and reduces the margin of error for safe operations.

All the above discussion contextualizes how the CRASH Clock can be used. It is not a strict limit - rather, it measures risk along a spectrum, with short CRASH Clock times representing a dangerous condition, moderate times representing a caution region, and long times indicating a healthy operational orbital environment. There is some degree of subjectivity in the boundaries of these "danger", "caution", and "safe" regions, but this makes the CRASH Clock adaptable without changing the underlying definition. As an illustrative example, and recalling our calculations above, our current CRASH Clock

value of $\tau_{\text{col}} = 5.5$ d corresponds to a 17% probability of one or more potential collisions during a 24 hour period of no manoeuvre conditions. We consider this to be well within the “caution” region. We could further (and arbitrarily) define the “danger” region to be where the CRASH Clock value implies a 50% chance of at least one potential collision within 24 hours. To stay in the “caution” region and below this “danger” threshold, the CRASH Clock value would therefore need to be longer than 1.4 d.

We could adopt smaller cross sections for the CRASH Clock, indicating when collisions are not just possible but probable. The 4.8m-2.4m-10cm Clock (see Methods) is one example, with a value of about 23 d. From a policy standpoint, however, there needs to be discussion concerning whether the Clock threshold should indicate possible or probable collisions. We have highlighted possible collisions not to be alarmists, but to contextualize the stress and demands on space safety.

Collision risk is not the only issue. We are already experiencing disruption of astronomy [37], pollution in the upper atmosphere from increasingly frequent satellite ablation [38], and increased ground casualty risks [39]. By these safety and pollution metrics, it is clear we have already placed substantial stress on LEO, and changes to our approach are required immediately.

We end by acknowledging that many different groups are working and collaborating to address these issues, especially collision risks. Satellite operators in particular are by no means idle in this regard, as it is in their interest to maintain a safe orbital environment and have teams dedicated to space safety and sustainability. The CRASH Clock is intended to be a tool to help with such efforts.

4 Methods

4.1 RSO density distribution

Number densities are calculated using the orbital information in the satellite catalogue as of 25 June 2025 for Figure 1, and again for 1 January 2018 for the historical comparison shown in Figure 2. We divide LEO into a series of spherical shells with 1 km radial widths. Within each shell, the total number of RSOs is counted and divided by the shell volume. To capture the effects of eccentric orbits, including those that have apogees higher than LEO, an RSO’s contribution to a given shell is weighted by the fraction of time per orbit that the RSO spends in that shell.

As noted in the main text, the resulting densities should be interpreted as averages, with some orbital configurations having significant density variations, such as the high densities that can occur near the maximum projected latitude excursions for inclined orbits. Our analytic/CRASH Clock calculations could potentially be improved by accounting for the actual distribution of inclinations. We leave this for future work, and do not think this changes the overall suitability of the CRASH Clock as a KEI.

The distribution of densities, and thus encounter rates, also evolve as objects are launched into orbit and satellite configurations change: we ran additional simulations (not shown here) for an October 2024 catalogue, and saw that the morphology of the

encounter distributions were different than that of 2025 (though the shortest encounter interval stayed about the same).

4.2 Typical Relative Speed Calculation

Assume that the orbits of objects in a shell are randomly oriented and circular. Under these assumptions, the encounter velocity between any two RSOs is

$$\vec{v}_r = v_o (\sin \theta \hat{x} + (1 - \cos \theta) \hat{y}), \quad (3)$$

where v_o is the circular orbital speed for the shell. We have oriented our frame of reference such that \hat{y} is one satellite's direction of motion, with θ representing the angle between the two satellites' directions of motion. The relative speed of the encounter is then

$$v_r = v_o (\sin^2 \theta + (1 - 2 \cos \theta + \cos^2 \theta))^{1/2} \quad (4)$$

$$= \sqrt{2} v_o (1 - \cos \theta)^{1/2}. \quad (5)$$

The average is calculated by integrating over all possible orientations. We assume that the angular momentum vectors are randomly distributed over a sphere (this is slightly different from assuming that the angle θ is randomly distributed). The resulting integration is thus

$$\bar{v}_r = \frac{\sqrt{2}}{2} v_o \int_0^\pi (1 - \cos \theta)^{1/2} \sin \theta d\theta \quad (6)$$

$$\bar{v}_r = \frac{4}{3} v_o. \quad (7)$$

At an altitude of about 550 km, the resulting typical relative speed between RSOs is about 10 km/s.

4.3 Collision Cross Sections

As an illustrative reference example only, in our result for possible collisions among LEO RSOs we assume that the collision cross section for satellite-satellite, rocket body-satellite, rocket body-rocket body, debris-satellite, debris-rocket body, debris-debris be 300, 300, 300, 79, 79, 0.03 m², respectively. These collisional areas, which are not the same as the individual cross section of each object, correspond to a close approach distance of 10 m between two satellites, satellite-rocket body, or two rocket bodies; 5 m between a satellite or rocket body and debris, and 10 cm between two pieces of debris. Again, this is only intended to be approximate, yet meaningful. These values are also used for determining the CRASH Clock in the main text, but this will need to be reevaluated as conditions and information change. In the article, we referred to this clock as the 10m-5m-10cm Clock. The motivation behind choosing these values is that they represent distances at which a collision could occur for many objects, depending on their orientation. These are thus close approach distances of serious concern – not guaranteed collisions.

Moreover, using the average area of a satellite could underestimate the collision potential. Take the Starlink V2 mini as an example, which has approximate dimensions of 0.3

$\text{m} \times 4.1 \text{ m} \times 29 \text{ m}$. The average surface area is approximately 43 m^2 . If the collision cross section between two objects is defined as $A_{\text{col}} = (A_1^{1/2} + A_2^{1/2})^2$, as is commonly done, the estimated collision cross section would be 61 m^2 . As discussed in the main text, two randomly oriented thin rods of full span L have a typical collision distance (between rod centres) of approximately $0.3L$. Thus, for the Starlink V2 minis, assuming random orientations, the effective collision cross section approaches the 300 m^2 value we use – the average area of the satellite vastly underestimates the collision potential in this case.

Nevertheless, we are mindful that not all objects will have such geometries, and as such, it is important to explore different Clocks. Based on the ESA environmental report [15] of average megaconstellation satellite surface areas, a rough estimate of collisional encounter distances is 4.8 m (i.e., a collision cross section of about 72 m^2). Thus, if we take close approaches of 4.8 m , 2.4 m , and 10 cm (in the same way as above) to lead to collisions, the resulting $4.8\text{m}-2.4\text{m}-10\text{cm}$ Clock is 23 d for 2025 and 701 d for 2018.

In short, the Clock value is dependent on assumptions of the minimum tolerable close approaches, but the trends highlighted by various Clocks are ultimately the same.

4.4 N-body Conjunction Simulation

We verify our analytic model against direct N-body conjunction simulations. Written in Python, the simulation code `SatEvol` propagates orbits using Keplerian orbital elements, and includes nodal and apsidal precession due to Earth's J_2 gravitational moment. Whenever objects are within a defined threshold distance of each other, for example, 1 km , those pairs are tracked until their separation is once again greater than the threshold. The TLEs for a given date are used for the initial conditions, consistent with those used for producing the density distributions in Figure 1. All RSOs are propagated to a common starting epoch using the Python implementation of the Simplified Gravitational Perturbations model (SGP-4) [40]. Minimum distances are determined using a k -dimensional tree search [41].

Postprocessing of simulation output is then used to identify each conjunction, along with its minimum encounter distance. We track objects according to their catalogue type, e.g., satellites, debris, and discarded rocket bodies, as well as specifically Starlink satellites due to their abundance. At this time, the code does not include additional perturbative effects (e.g. from the Sun and Moon, tesseral harmonics, radiation pressure, or atmospheric drag).

To capture these extremely fast close approaches, we use a time step of 0.05 seconds for the 1 km conjunction sims, and a step of 0.001 seconds for the 100 m conjunction sims.

5 Data Availability

All TLE data in this work are retrieved from <https://www.space-track.org/>.

6 Code Availability

The CRASH Clock is hosted at the public website <https://outerspaceinstitute.ca/crashclock>. The N-body simulation code used in this paper is open source and can be found at <https://github.com/norabolig/conjunctionSim>.

Software

This research was made possible by the open-source projects `Numba` [42], `Jupyter` [43], `iPython` [44], and `Matplotlib` [45].

References

- [1] Science and Technical Subcommittee of the Committee on the Peaceful Uses of Outer Space (S&T COPUOS): IADC space debris mitigation guidelines. Technical Report A/AC.105/C.1/2025/CRP.9, United Nations (2025)
- [2] ESA Space Debris Mitigation Working Group (ESA): ESA space debris mitigation requirements. Technical Report ESSB-ST-U-007 Issue 1, European Space Agency (2023)
- [3] IADC Steering Group and Working Group 4: IADC statement on large constellations of satellites in low earth orbit. Technical report, Inter-Agency Space Debris Coordination Committee (July 2021). https://iadc-home.org/documents_public/file_down/id/5253
- [4] Liou, J.-C., Johnson, N.L.: A leo satellite postmission disposal study using legend. *Acta Astronautica* **57**(2), 324–329 (2005) <https://doi.org/10.1016/j.actaastro.2005.03.002> . Infinite Possibilities Global Realities, Selected Proceedings of the 55th International Astronautical Federation Congress, Vancouver, Canada, 4-8 October 2004
- [5] Letizia, F., Lemmens, S., Bastida Virgili, B., Krag, H.: Application of a debris index for global evaluation of mitigation strategies. *Acta Astronautica* **161**, 348–362 (2019) <https://doi.org/10.1016/j.actaastro.2019.05.003>
- [6] D'Ambrosio, A., Linares, R.: Carrying capacity of low earth orbit computed using source-sink models. *Journal of Spacecraft and Rockets* (2024) <https://doi.org/10.2514/1.A35729> <https://doi.org/10.2514/1.A35729>
- [7] Parker, W., Brown, M., Linares, R.: Greenhouse gases reduce the satellite carrying capacity of low earth orbit. *Nature Sustainability* **8**, 363–372 (2025) <https://doi.org/10.1038/s41893-025-01512-0>
- [8] United Nations: Global indicator framework for the Sustainable Development Goals

and targets of the 2030 Agenda for Sustainable Development (2025). <https://unstats.un.org/sdgs/indicators/Global-Indicator-Framework-after-2025-review-English.pdf>

[9] Lawrence, A.: Astronomy, doughnuts, and carrying capacity. In: Astronomy and Satellite Constellations: Pathways Forward; IAU Symposium No. 385 (2023). <http://arxiv.org/abs/2311.09504>

[10] Lewis, H.: A space environment health situation report. In: 9th European Conference on Space Debris, vol. 9 (2025). <https://conference.sdo.esoc.esa.int/proceedings/sdc9/paper/274>

[11] Kessler, D.J., Cour-Palais, B.G.: Collision frequency of artificial satellites: The creation of a debris belt. *Journal of Geophysical Research* **83**(A6), 2637–2646 (1978) <https://doi.org/10.1029/JA083iA06p02637>

[12] Kelvey, J.: Understanding the misunderstood Kessler Syndrome (2024). <https://aerospaceamerica.aiaa.org/features/understanding-the-misunderstood-kessler-syndrome/>

[13] Soga, M., Gaston, K.J.: Shifting baseline syndrome: causes, consequences, and implications. *Frontiers in Ecology and the Environment* **16**(4), 222–230 (2018) <https://doi.org/10.1002/fee.1794> <https://esajournals.onlinelibrary.wiley.com/doi/pdf/10.1002/fee.1794>

[14] DQSII, Connie Walker (editor), Piero Benvenuti (editor): Dark and Quiet Skies II Working Group Reports. Zenodo (2022). <https://doi.org/10.5281/zenodo.5874725> . <https://doi.org/10.5281/zenodo.5874725>

[15] ESA Space Debris Office: ESA'S Annual Space Environment Report. European Space Agency (2025). https://www.esa.int/Space_Safety/Space_Debris/ESA_Space-Environment_Report_2025

[16] Letizia, F., Bastida Virgili, B., Lemmens, S.: Assessment of orbital capacity thresholds through long-term simulations of the debris environment. *Advances in Space Research* **72**(7), 2552–2569 (2023) <https://doi.org/10.1016/j.asr.2022.06.010> . Space Environment Management and Space Sustainability

[17] SpaceX: SpaceX gen1 and gen2 status report. Technical report, Space Exploration Technologies Corp. (2025)

[18] Liou, J.-C., Johnson, N.L.: Instability of the present LEO satellite populations. *Advances in Space Research* **41**(7), 1046–1053 (2008) <https://doi.org/10.1016/j.asr.2007.04.081>

[19] Lewis, H.G., Kessler, D.J.: Critical number of spacecraft in low earth orbit: a new assessment of the stability of the orbital debris environment. In: 9th European

Conference on Space Debris, pp. 1–4. ESA Space Debris Office, ??? (2025). <https://conference.sdo.esoc.esa.int/proceedings/sdc9/paper/305/SDC9-paper305.pdf>

[20] Thiele, S., Boley, A.C.: Investigating the Risks of Debris-Generating ASAT Tests in the Presence of Megaconstellations. *Journal of the Astronautical Sciences* **69**(6), 1797–1820 (2022) <https://doi.org/10.1007/s40295-022-00356-6> arXiv:2111.12196 [astro-ph.EP]

[21] Boley, A., Byers, M.: Anti-satellite weapon tests to disrupt large satellite constellations. *Nature Astronomy* **8**(1), 10–12 (2024) <https://doi.org/10.1038/s41550-023-02173-9>

[22] Çelikbilek, K., Simona Lohan, E., Praks, J.: Optimization of a leo-pnt constellation: Design considerations and open challenges. *International Journal of Satellite Communications and Networking* **43**(4), 272–292 (2025) <https://doi.org/10.1002/sat.1555> <https://onlinelibrary.wiley.com/doi/pdf/10.1002/sat.1555>

[23] Guan, M., Xu, T., Gao, F., Nie, W., Yang, H.: Optimal walker constellation design of leo-based global navigation and augmentation system. *Remote Sensing* **12**(11) (2020) <https://doi.org/10.3390/rs12111845>

[24] Cornara, S., Beech, T.W., Belló-Mora, M., Janin, G.: Satellite constellation mission analysis and design. *Acta Astronautica* **48**(5), 681–691 (2001) [https://doi.org/10.1016/S0094-5765\(01\)00016-9](https://doi.org/10.1016/S0094-5765(01)00016-9)

[25] National Oceanic and Atmospheric Administration Office (NOAA): The Legacy of the Exxon Valdez Oil Spill (2019). <https://response.restoration.noaa.gov/oil-and-chemical-spills/significant-incidents/legacy-exxon-valdez-oil-spill>

[26] Parker, W.E., Linares, R.: Satellite Drag Analysis During the May 2024 Gannon Geomagnetic Storm. *Journal of Spacecraft and Rockets* **61**(5), 1412–1416 (2024) <https://doi.org/10.2514/1.A36164> arXiv:2406.08617 [astro-ph.EP]

[27] Berger, T.E., Dominique, M., Lucas, G., Pilinski, M., Ray, V., Sewell, R., Sutton, E.K., Thayer, J.P., Thiemann, E.: The thermosphere is a drag: The 2022 starlink incident and the threat of geomagnetic storms to low earth orbit space operations. *Space Weather* **21**(3), 2022–003330 (2023) <https://doi.org/10.1029/2022SW003330> <https://agupubs.onlinelibrary.wiley.com/doi/pdf/10.1029/2022SW003330>. e2022SW003330 2022SW003330

[28] Parker, W.E., Freeman, M., Chisham, G., Kavanagh, A., Mun Siew, P., Rodriguez-Fernandez, V., Linares, R.: Influences of space weather forecasting uncertainty on satellite conjunction assessment. *Space Weather* **22**(7), 2023–003818 (2024) <https://doi.org/10.1029/2023SW003818> <https://agupubs.onlinelibrary.wiley.com/doi/pdf/10.1029/2023SW003818>.

- [29] Kyoto, Nose, M., Iyemori, T., Sugiura, M., Kamei, T., Matsuoka, A., Imajo, S., Kotani, T.: Geomagnetic dst index. Technical report, World Data Center for Geomagnetism (2015). <https://wdc.kugi.kyoto-u.ac.jp/wdc>
- [30] Cliver, E.W., Dietrich, W.F.: The 1859 space weather event revisited: limits of extreme activity. *J. Space Weather Space Clim.* **3**, 31 (2013) <https://doi.org/10.1051/swsc/2013053>
- [31] Green, J.L., Boardsen, S.: Duration and extent of the great auroral storm of 1859. *Advances in Space Research* **38**(2), 130–135 (2006) <https://doi.org/10.1016/j.asr.2005.08.054> . The Great Historical Geomagnetic Storm of 1859: A Modern Look
- [32] Pultarova, T.: SpaceX Starlink satellites had to make 25,000 collision-avoidance maneuvers in just 6 months — and it will only get worse (2023). <https://www.space.com/starlink-satellite-conjunction-increase-threatens-space-sustainability>
- [33] Pultarova, T.: Performing evasive maneuvers increases satellites' collision risk down the road (2023). <https://www.space.com/satellites-collision-avoidance-maneuvers-increase-collision-risk>
- [34] Boyle, A.: SpaceX reports a ‘bug’ in its alert system after ESA shifts spacecraft to avoid Starlink satellite collision (2019). <https://www.geekwire.com/2019/esa-shifts-spacecraft-avoid-starlink-satellite-spacex-reports-bug-collision-warning-system/>
- [35] Shepperd, R.: Subsequent Assessment of the Collision between Iridium 33 and COSMOS 2251. In: AMOS Tech (2023). <https://amostech.com/TechnicalPapers/2023/Conjunction-RPO/Shepperd.pdf>
- [36] United Nations Office of Outer Space Affairs (UNOOSA): Guidelines for the Long-term Sustainability of Outer Space Activities of the Committee on the Peaceful Uses of Outer Space (2021). https://www.unoosa.org/documents/pdf/PromotingSpaceSustainability/Publication_Final_English_June2021.pdf
- [37] Lawrence, A., Rawls, M.L., Jah, M., Boley, A., Di Vrudo, F., Garrington, S., Kramer, M., Lawler, S., Lowenthal, J., McDowell, J., McCaughean, M.: The case for space environmentalism. *Nature Astronomy* **6**, 428–435 (2022) <https://doi.org/10.1038/s41550-022-01655-6> arXiv:2204.10025 [astro-ph.IM]
- [38] Murphy, D.M., Abou-Ghanem, M., Cziczo, D.J., Froyd, K.D., Jacquot, J.L., Lawler, M., Maloney, C., Plane, J.M.C., Ross, M., Schill, G.P., Shen, X.: Metals from the reentry of spacecraft in stratospheric particles. In: AGU Fall Meeting Abstracts, vol. 2023, pp. 32–01 (2023). <https://doi.org/10.1073/pnas.2313374120>

- [39] Wright, E., Boley, A., Byers, M.: Airspace closures due to reentering space objects. *Scientific Reports* **15**(1), 2966 (2025) <https://doi.org/10.1038/s41598-024-84001-2>
- [40] Vallado, D., Crawford, P., Hujasak, R., Kelso, T.S.: Revisiting spacetrack report #3: Rev 1. In: AIAA/AAS Astrodynamics Specialist Conference and Exhibit (2006). <https://doi.org/10.2514/6.2006-6753>
- [41] Maneewongvatana, S., Mount, D.M.: Analysis of approximate nearest neighbor searching with clustered point sets. In: ALENEX '99, Baltimore (1999). <https://arxiv.org/abs/cs/9901013>
- [42] Lam, S.K., Pitrou, A., Seibert, S.: Numba: a llvm-based python jit compiler. In: Proceedings of the Second Workshop on the LLVM Compiler Infrastructure in HPC. LLVM '15. Association for Computing Machinery, New York, NY, USA (2015). <https://doi.org/10.1145/2833157.2833162>
- [43] Granger, B.E., Pérez, F.: Jupyter: Thinking and storytelling with code and data. *Computing in Science & Engineering* **23**(2), 7–14 (2021) <https://doi.org/10.1109/MCSE.2021.3059263>
- [44] Pérez, F., Granger, B.E.: IPython: a system for interactive scientific computing. *Computing in Science and Engineering* **9**(3), 21–29 (2007) <https://doi.org/10.1109/MCSE.2007.53>
- [45] Hunter, J.D.: Matplotlib: A 2d graphics environment. *Computing in Science & Engineering* **9**(3), 90–95 (2007) <https://doi.org/10.1109/MCSE.2007.55>

7 Acknowledgments

We thank Christopher Chyba and Ryne Beeson for helpful discussions regarding our simulation code and the relative velocity calculation. We also thank Hugh Lewis for comments that improved this manuscript.

8 Author Contributions

All authors were fully involved in all aspects of this research. ST wrote the initial draft. FUNDING Natural Sciences and Engineering Research Council of Canada DH-2022-00477 (AB, SH) and RGPIN-2020-04111 (SL)

9 Competing interests

Authors have no competing interests to declare.

10 Supplementary information

There is no supplementary material for this work.